Frontiers in Bioscience Landmark

Front. Biosci. (Landmark Ed) **2022**; 27(9): 275
https://doi.org/10.31083/j.fbl2709275

Original Research

Exosomal miR-22-3p from Mesenchymal Stem Cells Inhibits the Epithelial-Mesenchymal Transition (EMT) of Melanoma Cells by Regulating *LGALS1*

Yong Chen[1,†], Yuan Fang[2,3,†], Li Li[4], Hui Luo[5,*], Tianran Cao[6,*], Biao Tu[7,*]

[1]Department of Plastic Surgery and Dermatology, The First Hospital of Changsha, 410005 Changsha, Hunan , China
[2]Department of Plastic and Reconstructive Surgery, Shanghai Ninth People's Hospital, Shanghai Jiao Tong University School of Medicine, 200011 Shanghai, China
[3]Department of Plastic Surgery, The Third Xiangya Hospital, Central South University, 410008 Changsha, Hunan, China
[4]Department of Cosmetic and Plastic Surgery, Yueyang Central Hospital, 414000 Yueyang, Hunan, China
[5]Department of Cardiology, The First Hospital of Changsha, 410005 Changsha, Hunan, China
[6]Office of the Drug Clinical Trail Organization, The First Hospital of Changsha, 410005 Changsha, Hunan, China
[7]Department of Cardiothoracic Surgery, The First Hospital of Changsha, 410005 Changsha, Hunan, China
*Correspondence: huihui667013@163.com (Hui Luo); naturenew@163.com (Tianran Cao); tubiao0803@163.com (Biao Tu)
[†]These authors contributed equally.

Academic Editor: Qing Ye
Submitted: 11 July 2022 Revised: 27 September 2022 Accepted: 28 September 2022 Published: 29 September 2022

Abstract

Background: The mortality rate from melanoma has been rising and hence new therapeutic approaches for this disease have received extensive attention, especially the search for novel therapeutic targets. The aim of this study was to find new targets for the treatment of melanoma through a bioinformatics and experimental approach. **Methods**: First, we screened for differentially expressed genes (DEGs) and differentially expressed miRNAs (DEMs) between melanoma and normal tissues using the TCGA-SKCM, GTEX, and GSE24996 datasets. Next, we identified epithelial-mesenchymal transition (EMT)-related DEGs and analyzed their expression levels and association with patient survival. The expression level of DEGs was then confirmed in normal human melanocytes and melanoma cells. Bioinformatics analysis was used to identify miRNAs that targeted the most highly expressed DEG, *LGALS1*, and their binding confirmed using dual luciferase. Enriched pathways for the *LGALS1* target miR-22-3p were also analyzed. miR-22-3p was overexpressed in cells in order to investigate changes in cell activity and in related genes and proteins. Exosomes from human bone marrow mesenchymal stem cells (MSCs) were coated with miR-22-3p to examine its effect on EMT. **Results**: The expression levels of *LGALS1*, *CPXM1*, and *APLNR* were higher in melanoma than in normal tissues and were associated with worse patient survival. The differential expression of these genes was confirmed using normal human skin melanocytes (PIG1) and human melanoma cells (WM-266-4). *LGALS1* was the most differentially expressed gene between WM-266-4 and PIG1 cells, and was also predicted to be a target for miR-22-3p. The results of dual luciferase experiments confirmed that miR-22-3p could bind to *LGALS1*. Following the overexpression of miR-22-3p in WM-266-4 cells, the cell viability decreased, the expression levels of *LGALS1*, *VIM* and *SNAI2* decreased, the expression level of *CDH1* increased, and cell apoptosis increased. Transfection of miR-22-3p using exosomes resulted in similar effects. **Conclusions**: We identified three genes (*LGALS1*, *CPXM1*, *APLNR*) that showed a high level of differential expression in melanoma. *LGALS1* is a target for miR-22-3p binding and this can inhibit the EMT of melanoma cells, thereby preventing the development of melanoma. Moreover, exosomes secreted by MSCs can be loaded with miR-22-3p, thus regulating the EMT process in melanoma cells.

Keywords: melanoma; epithelial-mesenchymal transition; *LGALS1*; miR-22-3p

1. Introduction

Melanoma is a highly malignant tumor [1] and in recent years its incidence and mortality have gradually increased [2]. Although some progress has recently been made with targeted therapy and immunotherapy for cutaneous melanoma, many patients still develop treatment resistance [3]. Therefore, the discovery of potential new targets for cutaneous melanoma should help to achieve further progress in the prevention and treatment of this disease.

The cell regulatory roles of miRNAs in melanoma have been extensively studied over the past decades [4]. miRNAs have been implicated in complex cell regulation processes involving gene expression and protein translation [4]. Targeted therapy based on miRNA has achieved good results in previous studies. However, due to the heterogeneity and multiple subtypes of cancer, the challenge for miRNA approaches is to identify the correct target [5]. Exosomes are vesicles secreted by cells that contain a variety of functional biological small molecules, including miRNAs, long non-coding RNAs (lncRNAs), and proteins [6]. miRNAs from exosomes can affect tumor immunity and the microenvironment to hinder cancer progression, thus further strengthening the therapeutic applications of certain miR-

NAs [6]. Exosomes secreted by human bone marrow mesenchymal stem cells (MSCs) have shown great potential for the treatment of tumors and inflammatory diseases. These have attracted widespread interest because of their ability to precisely localize to tumor cells [7].

Multiple miRNAs have been shown to be involved in regulating the epithelial-mesenchymal transition (EMT) in melanoma [8,9]. EMT is commonly observed when epithelial tumor cells transform into mesenchymal cells, thereby leading to tumor metastasis and therapy resistance [10]. EMT-inducing transcription factors play an important role in the transition of melanocytes into malignant melanoma [11]. EMT also allows the proliferative, migratory, and invasive phenotype of melanoma cells to be transformed into mesenchymal cells, thus affecting their response to treatment [12–14]. The goal of treating melanoma has therefore led to a search for melanoma-targeting miRNAs and for genes related to EMT.

Advanced bioinformatics analysis can provide novel insights into the prevention and treatment of various diseases [15]. Bioinformatics is also an effective tool for identifying relevant genes and targets in melanoma, and for analyzing possible associations between them. The aim of the present study was to use bioinformatics analysis to identify genes and miRNAs associated with melanoma metastasis, prognosis, and EMT. We also conducted *in vitro* experiments to confirm that the identified genes and miRNAs play a role in melanoma. By combining bioinformatics with experimental methods, we have discovered new targets that may be relevant to melanoma. The EMT of melanoma cells was found to be regulated by miRNAs contained within exosomes secreted by MSCs. The present study could therefore provide novel insights for the treatment of melanoma.

2. Materials and Methods

2.1 Dataset Selection for Bioinformatics Analysis

The TCGA-SKCM dataset was selected from the Cancer Genome Atlas (TCGA) database (https://portal.gdc.cancer.gov) and contains 469 melanoma tissue samples. Normal skin tissue samples (n = 813) were selected from the Genotype-Tissue Expression Project (GTEX, https://www.gtexportal.org/). GSE24996 was selected from the Gene Expression Omnibus (GEO) database (https://www.ncbi.nlm.nih.gov/geo/) and contains 15 melanoma tissue samples and 8 benign nevi samples.

2.2 Identification of DEGs

The Agilent platform was leveraged to generate raw data from the GEO database. Background correction and normalization were achieved using a robust multi-chip averaging (RMA) algorithm. The TCGA and GTEX databases provided RNA sequencing data. Fragment per kilobase (FPKM) values were converted to transcript per kilobase (TPM) values with signal intensities similar to RMA-treated values. Following normalization, data were analyzed using the limma package in R language. The screening standards for miRNA were $|\log FC| > \log_2 1.5$ and $p < 0.05$. The gene screening standards were $|\log FC| > 1$ and $p < 0.05$. Volcano plots were used to show all miRNAs and genes. The heatmap showed the top 45 differentially expressed miRNAs (DEMs) and the top 89 EMT-related DEGs. FPKM values were converted to TPM values with signal intensities similar to RMA-treated values.

2.3 Correlation Analysis

Correlation analyses were performed between DEGs and EMT. EMT hallmark gene sets were downloaded from the MSigDB database. For the TCGA-SKCM gene expression profile, the enrichment score for the HALLMARK_EPITHELIAL_MESENCHYMAL_TRANSITION pathway was calculated using Genomic Variation Analysis (GSVA) and EMT activity was assessed using the GSVA R package. DEGs that were significantly associated with this pathway were then identified. Correlation coefficients of >0.3 were considered to show a correlation between DEGs and EMT. These are detailed in **Supplementary Table 1**.

2.4 Survival Analysis

Survival analysis for 89 EMT-related genes was performed using the Kaplan-Meier method and the R language survival package. Cox regression was used to test significance, with $p < 0.05$ considered statistically significant.

2.5 Identification of miRNAs that Target DEGs

The R multiMiR package was used to identify miRNAs that target galectin 1 (*LGALS1*) in the pita, diana, and targetscan databases. Venn diagrams were used to display common miRNAs present in the three databases.

2.6 Gene Ontology (GO) Analysis and Kyoto Encyclopedia of Genes and Genomes (KEGG) Pathway Enrichment Analysis

The multiMiR package was used to search for genes targeted by miR-22-3p. The R language clusterProfiler package was then used for GO and KEGG enrichment pathway analysis.

2.7 Cell Culture and Group Processing

Normal human skin melanocytes (PIG1) and human melanoma cells (WM-266-4) originated from Shanghai Zeye Biotechnology Co., Ltd. MSCs originated from iCell Bioscience Inc. Both PIG1 and WM-266-4 cells were cultured in DMEM (D5796-500ML, SIGMA) with 10% fetal bovine serum and 1% penicillin-streptomycin. MSCs were cultured in a special medium (human bone marrow MSC complete medium, CM-H166, Procell) for primary MSCs. WM-266-4 cells were separated into three groups: cells in the control group did not undergo any treatment; cells in the mimics NC group were transfected with mimics NC plasmid; cells in the miR-22-3p mimics group were transfected

with miR-22-3p mimics plasmid. MSCs were divided into two groups. In the MSCs group, MSCs were cultured normally and the cells collected for evaluation. In the MSC-exos group, MSCs were cultured in serum-free medium, the cell supernatant was then collected and the exosomes extracted. In addition, MSCs were first transfected with mimics NC plasmids and miR-22-3p mimics plasmids, and the cell supernatant subsequently collected for the extraction of exosomes. WM-266-4 cells were divided into four groups. In the NC group, WM-266-4 cells were cultured normally. In the MSC-exos group, MSC-exos were added to the WM-266-4 cells for 12 h. In the MSC-exos$^{\text{mimics NC}}$ group, WM-266-4 cells were treated with exosomes secreted from MSCs that had previously been transfected with mimics NCs for 12 h. In the MSC-exos$^{\text{miR-22-3p mimics}}$ group, WM-266-4 cells were treated with exosomes secreted from MSCs that had previously been transfected with miR-22-3p mimics for 12 h. The plasmid transfection steps were: 5 μL mimics NC and 5 μL miR-22-3p mimics plasmids were added to 95 μL of basal medium, mixed gently, and allowed to stand for 5 min. Five μL of Lipofectamine 2000 (11668019, ThermoFisher) was added to 95 μL of basal medium. The plasmid and Lipofectamine 2000 were mixed separately and after standing for 20 min, 200 μL of mixture and 800 μL of basal medium were added to the cells. The medium was replaced by fresh complete medium after 6 h. Cells and cell supernatant were collected after 48 h for subsequent evaluation. All plasmids were obtained from Genechem Co., Ltd.

2.8 Extraction and Labeling of Exosomes

MSCs were cultured with serum-free medium for 2 days. The cell supernatant was then collected, centrifuged at 3500 rpm for 15 min, and the pellet discarded. The cell supernatant was mixed with ExoQuick exosome precipitation solution (EXOQ20A-1, System Biosciences Inc., USA) at a ratio of 5:1 and incubated at 4 °C overnight. The mixture was then centrifuged at 2500 rpm for 30 min, with the exosomes contained in the resulting pellet. Two uL of PKH67 reagent (Fluorescence, China) was then added to the resuspended exosomes and incubated at 37 °C for 20 min. Ten uL of serum was added to stop marking. WM-266-4 cells were treated with 100 uL of labeled exosomes and incubated at 37 °C for 1 h. After discarding the medium, cells were washed 3 times with Phosphate Buffered Saline (PBS) and fixed with paraformaldehyde. Nuclei were stained by adding 1 mg/mL of 4',6-diamidino-2-phenylindole (DAPI) working solution (AWC0291a, Abiowell) for 10 min at 37 °C. Confocal fluorescence microscopy was used to observe the cells after washing with PBS.

2.9 Dual Luciferase Experiments

TargetScan v.7.0 was used to predict the binding site between *LGALS1* and miR-22-3p (http://www.targetscan.org/vert_70/). Plasmid constructs were purchased from HonorGene. The pHG-MirTarget-*LGALS1* WT-3U and pHG-MirTarget-*LGALS1* MUT-3U plasmids were transfected into 293A cells seeded in 12-well plates. Subsequently, the miR-22-3p mimics plasmid and its empty vector mimics-NC were transfected into 293A cells. Each set of experiments was repeated three times. The activities of firefly luciferase and Renilla luciferase in each group were detected sequentially according to the instructions for the dual luciferase detection kit.

2.10 Western Blots

Cells were lysed on ice using Radio Immunoprecipitation Assay (RIPA) lysis buffer (AWB0136, Abiowell). The cell and lysate mixture was then centrifuged at 12,000 rpm for 15 min. The bicinchoninic acid (BCA) protein kit (AWB0104a, Abiowell) was used to measure protein concentrations. The marker and the denatured protein were mixed with loading buffer and subjected to agarose gel electrophoresis for 2 h. After cutting the gel according to molecular weight, the proteins were transferred to PVDF membranes. The membranes were blocked with 5% skimmed milk powder for 90 min at room temperature. Next, the membranes were incubated overnight at 4 °C with primary antibodies to CD63 protein (CD63) (25682-1-AP, proteintech, US), Heat Shock Protein Family A (Hsp70) Member 4 (HSPA4) (25405-1-AP, proteintech, US), galectin 1 (LGALS1) (11858-1-AP, proteintech, US), carboxypeptidase X, M14 family member 1 (CPXM1) (orb467709, biorbyt, UK), apelin receptor (APLNR) (20341-1-AP, proteintech, US), Vimentin (VIM) (10366-1-AP, proteintech, US), snail family transcriptional repressor 2 (SNAI2) (12129-1-AP, proteintech, US), cadherin 1 (CDH1) (20874-1-AP, proteintech, US), actin beta (ACTB) (66009-1-Ig, proteintech, US). ACTB was used as an internal control parameter. The membranes were then incubated with the corresponding secondary antibodies HRP goat anti-mouse IgG (SA00001-1, proteintech, US) and HRP goat anti-rabbit IgG (SA00001-2, proteintech, US) for 90 min at room temperature. Enhanced chemiluminescence (ECL) solution (AWB0005a, Abiowell) was used to reveal the bands, which were then photographed using a gel imaging system.

2.11 Real-Time Quantitative PCR (qRT-PCR)

Total RNA was extracted from cells according to instructions for the Trizol kit (15596026, Thermofisher). miRNA and mRNA were then transcribed into cDNA according to instructions for the miRNA cDNA Synthesis Kit (CW2141, Cowin bio.) and the HiFscript cDNA Synthesis Kit (CW2569, Cowin bio.), respectively. Primer 5.0 software (PREMIER Biosoft, San Francisco, California, USA) was used to design primers, which were then synthesized by Beijing Qingke Biotechnology. The primer sequences are shown in Table 1. Next, the primers were added to cDNA, ddH_2O, and the UltraSYBR Mixture (CW2601,

Cowin bio.). qRT-PCR was performed using *ACTB* as the internal reference for mRNA and *RNU6V* as the internal reference for miRNA. The qRT-PCR amplification program was: 95 °C for 10 min (pre-denaturation), 95 °C for 15 s, and 60 °C for 30 s (denaturation, annealing, and extension; 40 cycles in total). Preliminary experiments confirmed that the efficiency of all primers was between 90–110%. Samples were tested in triplicate and the $2^{-\triangle\triangle ct}$ method was used to analyze experimental data.

Table 1. Primer sequences.

Primer ID	5'-3'
ACTB-F	ACCCTGAAGTACCCCATCGAG
ACTB-R	AGCACAGCCTGGATAGCAAC
RNU6V-F	CTCGCTTCGGCAGCACA
RNU6V-R	AACGCTTCACGAATTTGCGT
LGALS1-F	TCGGGTGGAGTCTTCTGACA
LGALS1-R	ACGAAGCTCTTAGCGTCAGG
CPXM1-F	GCTGACCTCAACACACCACT
CPXM1-R	CATTCATGCCCCCGTGGAG
APLNR-F	GATGCCTGCCTCTTGTCTGT
APLNR-R	ATCCAGTAGGGGGTGGACTC
VIM-F	CCCTTGACATTGAGATTGCCACC
VIM-R	ACCGTCTTAATCAGAAGTGTCCT
CDH1-F	ATTTTTCCCTCGACACCCGAT
CDH1-R	TCCCAGGCGTAGACCAAGA
SNAI2-F	GCTACCCAATGGCCTCTCTC
SNAI2-R	CTTCAATGGCATGGGGGTCT
miR-22-3p-F	GCTGAGCCGCAGTAGTTCTT
miR-22-3p-R	GGCAGAGGGCAACAGTTCTT

2.12 Cell Counting Kit 8 (CCK8)

The cells in different groups were digested, counted, and seeded into 96 well plates at a density of 1×10^4 cells/well. Three wells were used for each group. Following specific treatment of the different groups, the culture medium was discarded and 10 μL of CCK8 working solution (NU679, Dojindo) and 90 μL of complete medium were added to each well. The cells were incubated at 37 °C for 4 h and a Bio Tek microplate reader was then used to measure the absorbance at 450 nm.

2.13 Flow Cytometry

Cells were grouped and then digested with trypsin, with PBS used as a washing agent. Experiments were performed strictly according to instructions for the Annexin V-APC/PI Apoptosis Detection Kit (KeyGEN BioTECH, KGA1030). Briefly, 500 uL of binding buffer was used to suspend the cells prior to testing, followed by the addition of 5 uL Annexin V-APC and 5 uL of propidium iodide. The mixture was left to stand for 10 min at room temperature and protected from light. Flow cytometry was then used for the measurement of fluorescence.

2.14 Statistical Analysis

All cell experiments were conducted in triplicate. Data for each group are shown as the mean $\pm$ standard deviation (SD) and were analyzed using Graphpad Prism 9.0 (GraphPad Software LLC, San Diego, California, USA). Student's *t*-test was used to compare two data groups, while ordinary one-way ANOVA was used to compare three data groups. $p < 0.05$ was considered statistically significant.

3. Results

3.1 Screening for DEMs and DEGs

The TCGA-SKCM and GTEX datasets were screened to identify DEGs between the melanoma and control groups, while data from the GSE24996 dataset was screened to identify DEMs between these groups. All DEMs (Fig. 1A) and DEGs (Fig. 1B) are shown in the volcano plot, while the heatmap shows the top 45 DEMs (Fig. 1C). DEMs included miR-211-5p, miR-205-5p, miR-125b-5p, miR-200c-3p, miR-768-3p, and miR-22-3p.

3.2 Survival Analysis for DEGs Associated with EMT

The 89 EMT-related DEGs are shown in the heatmap (Fig. 2A), and their correlation coefficients shown in **Supplementary Table 1**. EMT-related DEGs included *ADAM19*, *ITGAM*, *DCSTAMP*, *PLAUR*, *CSF3R*, *LGALS1*, *CPXM1*, and *APLNR*. Survival analysis was performed according to the expression of each of these 89 genes. Kaplan-Meier analysis showed that expression of three genes (*LGALS1*, *CPXM1*, *APLNR*) was significantly associated with patient survival. Low gene expression in the tumor tissue correlated with better patient survival (Fig. 2B). Next, Boxplots were drawn based on the expression level of these three genes in the melanoma and control groups. These showed that the expression of all three genes was higher in the melanoma group compared to the control group (Fig. 2C).

3.3 LGALS1 is Highly Expressed in Melanoma Cells

To confirm the observed differences in expression of the above three DEGs, we compared the expression levels of the *LGALS1*, *CPXM1*, and *APLNR* genes (Fig. 3A) and the LGALS1, CPXM1, and APLNR proteins (Fig. 3B) between PIG1 and WM-266-4 cells. Both the mRNA and protein levels for all three DEGs were significantly higher in WM-266-4 cells than in PIG1 cells, with the difference being greatest for LGALS1.

3.4 LGALS1-Interacting miRNAs

LGALS1 was selected for the follow-up research because it showed the most difference in expression between melanoma and control. Three databases (pita, diana, and targetscan) were used to identify miRNAs predicted to target *LGALS1*. Only one miRNA, miR-22-3p, was found in all three databases to target *LGALS1*, as shown by Venn

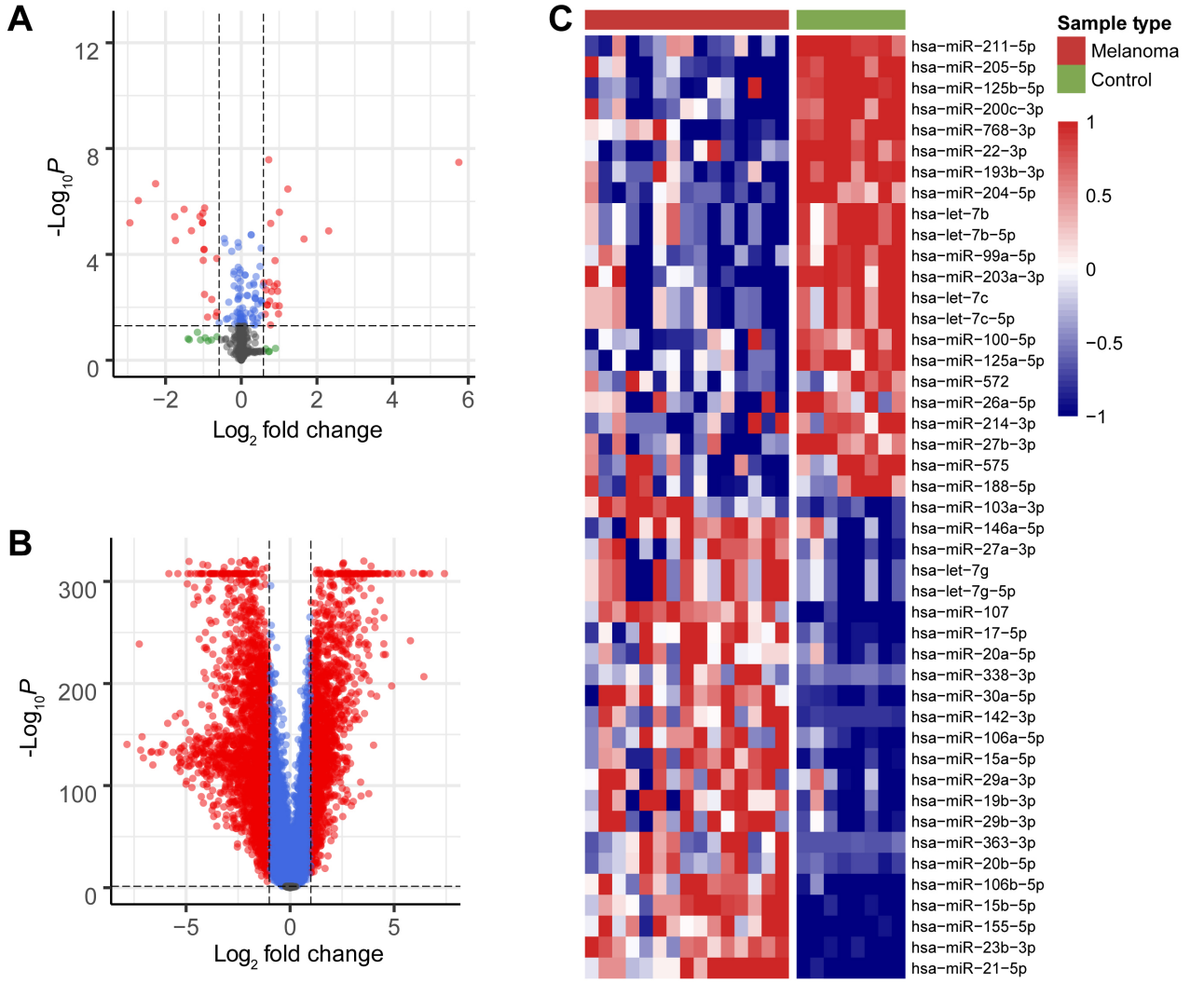

Fig. 1. Screening for DEMs and DEGs. (A) Volcano plot of all miRNAs that were differently expressed between the melanoma and control groups in the GEO database. (B) Volcano plot of all mRNAs that were differently expressed between the melanoma and control groups in the TCGA and GTEX databases. Red dots indicate significant up-regulation and down-regulation of DEMs and DEGs between the two groups ($|\log FC| > \log_2 1.5$, p-value < 0.05). (C) Heatmap showing the top 45 DEMs between the melanoma and control groups. Darker red indicates higher expression, while darker blue indicates lower expression.

diagram (Fig. 4A). Boxplots showed that the expression of miR-22-3p in the melanoma group was lower than in the control group (Fig. 4B). Next, GO analysis and KEGG analysis were performed (Fig. 4C). GO analysis showed that in biological processes (BP), *LGALS1*-targeted miR-22-3p was significantly associated with endocytosis, platinum drug resistance, the sphingolipid signaling pathway, the AMPK signaling pathway, and proteoglycans in cancer. In cellular components (CC), *LGALS1*-targeted miR-22-3p bound to proximal promoter sequence-specific DNA binding, protein serine/threonine kinase activity, transcription cofactor binding, RNA polymerase II proximal promoter sequence-specific DNA binding, and enzyme activator activity. For molecular function (MF), *LGALS1*-targeted miR-22-3p was related to the dendritic spine, neuron spine, spindle, main axon, and cell leading edge. The KEGG signaling pathway was mainly enriched in learning or memory, cognition, regulation of GTPase activity, cell morphogenesis involved in neuron differentiation, regulation of cell morphogenesis, and regulation of neuron death. Next, qRT-PCR was used to confirm the expression of miR-22-3p in cells. The miR-22-3p level in PIG1 cells was higher than in WM-266-4 cells (Fig. 4D). The targeted binding of miR-22-3p to *LGALS1* was predicted by LncBase Predicted v.2 (Fig. 4E) and confirmed using a dual luciferase experiment (Fig. 4F). The results demonstrated that miR-22-3p targeted *LGALS1*.

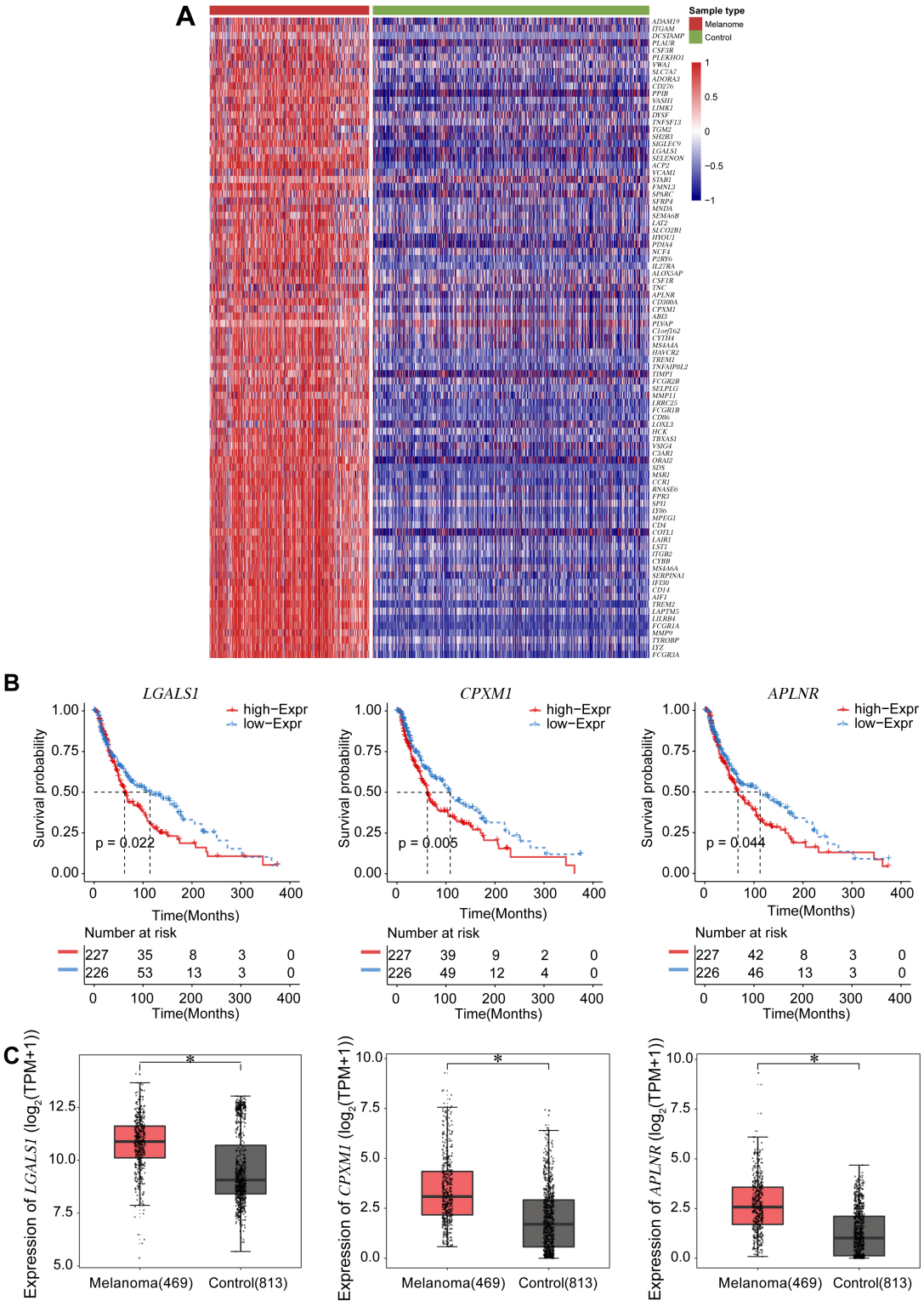

Fig. 2. Survival analyses for the expression of three DEGs associated with EMT. (A) Heatmap of 89 DEGs identified from the TCGA and the GTEX databases and associated with EMT. Darker red corresponds to higher expression and darker blue corresponds to lower expression. (B) Survival curves according to expression of the DEGs *LGALS1*, *CPXM1*, and *APLNR*. The red line represents the survival probability of patients with high gene expression, while the blue line represents the survival probability of patients with low gene expression. (C) Boxplots show the expression level of the three DEGs *LGALS1*, *CPXM1*, and *APLNR* in the melanoma and control groups. *$p < 0.05$ Melanoma group vs. Control group.

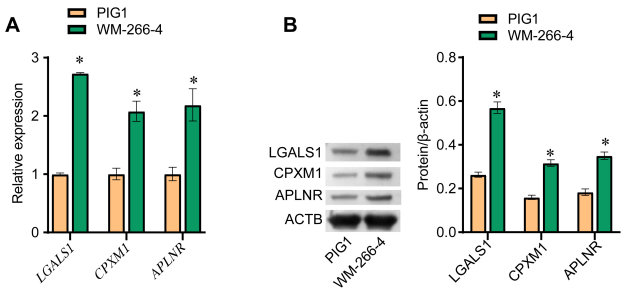

Fig. 3. LGALS1 is highly expressed in melanoma cells. (A) qRT-PCR was performed to evaluate *LGALS1*, *CPXM1* and *APLNR* mRNA expression in PIG1 and WM-266-4 cells. (B) Western blot was used to evaluate the expression of LGALS1, CPXM1 and APLNR protein in PIG1 and WM-266-4 cells. *$p < 0.05$ WM-266-4 cells vs. PIG1 cells.

3.5 miR-22-3p Regulates EMT in Melanoma Cells

The effect of miR-22-3p on EMT was investigated by overexpressing miR-22-3p in WM-266-4 cells. The qRT-PCR result showed that the expression of miR-22-3p in the miR-22-3p mimics group was significantly higher than in the mimics NC group, indicating successful overexpression of miR-22-3p in WM-266-4 cells (Fig. 5A). Cell viability was found to decrease significantly following the overexpression of miR-22-3p (Fig. 5B). In addition, flow cytometry showed that cell apoptosis increased after transfection with miR-22-3p mimics (Fig. 5D). The mRNA expression level of LGALS1 and other EMT-related genes (*CDH1*, *VIM*, and *SNAI2*), together with their protein expression level, was examined by qRT-PCR and western blot, respectively (Fig. 5C,E). The expression levels of *LGALS1* and LGALS1 were significantly lower in the miR-22-3p mimics group than in the mimics NC group. Furthermore, the expression of *LGALS1* and LGALS1 was negatively correlated with miR-22-3p. The expression of *CDH1* and CDH1 was significantly higher in the miR-22-3p mimics group than in the mimics NC group, while the mRNA expression levels for *VIM*, VIM, *SNAI2*, and SNAI2 were significantly lower in the miR-22-3p mimics group. These results indicate that miR-22-3p can inhibit EMT.

3.6 Identification of MSC-EXOs and Uptake of Exosomes by Melanoma Cells

The exosomes secreted by MSCs were isolated and observed by transmission electron microscopy (TEM) to be round vesicles with a diameter of about 50 nm (Fig. 6A). Western blot assay was used to detect the exosome-associated proteins CD63 and HSPA4. Both proteins were expressed in the MSC-exos group (Fig. 6B). Next, PCR revealed that miR-22-3p expression was higher in the MSC-exos group than in the MSC group (Fig. 6C). These results indicate that exosomes secreted by MSCs contain a large amount of miR-22-3p. The uptake of exosomes by WM-266-4 cells was observed by confocal fluorescence microscopy (Fig. 6D).

3.7 miR-22-3p in MSC-exos Inhibits the EMT of Melanoma Cells by Regulating LGALS1

The amount of miR-22-3p in each cell group was evaluated. The expression of miR-22-3p in the MSC-exos$^{\text{miR-22-3p mimics}}$ group was significantly higher than in the MSC-exos$^{\text{mimics NC}}$ group (Fig. 7A), demonstrating that miR-22-3p was successfully overexpressed in exosomes. Next, the CCK8 assay was used to measure the proliferative activity of each cell group. The proliferation of cells in the MSC-exos group was slower than that of cells in the NC group (Fig. 7B). In contrast, the proliferation of cells in the MSC-exos$^{\text{miR-22-3p mimics}}$ group was slower than that of cells in the MSC-exos$^{\text{mimics NC}}$ group. This results indicates that miR-22-3p in exosomes secreted by MSC-exos can inhibit the proliferation of WM-266-4 cells. Furthermore, flow cytometry showed that exosomes carrying miR-22-3p can promote cell apoptosis (Fig. 7C). The expression levels of *LGALS1*, LGALS1, *VIM*, VIM, *SNAI2*, and SNAI2 in cells from the MSC-exos group were significantly lower than in the NC group, whereas the expression level of *CDH1* and CDH1 in MSC-exos$^{\text{miR-22-3p mimics}}$ cells was significantly increased (Fig. 7D,E). The expression levels of *LGALS1*, LGALS1, *VIM*, VIM, *SNAI2*, and SNAI2 in MSC-exos$^{\text{miR-22-3p mimics}}$ cells were significantly lower compared to the MSC-exos$^{\text{mimics NC}}$ group, whereas the expression of *CDH1* and CDH1 in MSC-exos$^{\text{miR-22-3p mimics}}$ cells was significantly increased.

4. Discussion

Melanoma is a rare primary skin tumor [16]. Melanoma has a high incidence and a poor prognosis [16]. Therefore, considerable effort is still required to find novel targets for melanoma that lead to early diagnosis and new treatments.

In recent years, bioinformatics has greatly improved the efficiency of target prediction for various diseases [17]. Bioinformatics analysis was used here to screen large databases for DEGs and for predicting the biological functions of candidate targets [18]. By downloading data on ovarian cancer from the GEO database, Yang *et al.* [19] identified 62 candidate small molecules associated with this disease. These could be used as potential targets for novel drugs to treat ovarian cancer [19]. More recently, bioinformatics analysis has also been widely used in melanoma research. Wang *et al.* [20] used bioinformatics analysis to construct a melanoma ceRNA network. These authors identified 5 miRNAs (miRNA-29c, miRNA-100, miR-142-3p, miR-150, miR-516a-2), 6 lncRNAs (lncRNA AC068594.1, C7orf71, FAM41C, GPC5-AS1, MUC19, LINC00402) and 7 mRNAs (*CCDR9*, *CNR2*, *DIRAS2*, *ESRP2*, *FAM83C*, *KCNT2*, *USH1G*) that were aberrantly expressed in melanoma [20]. They postulated their find-

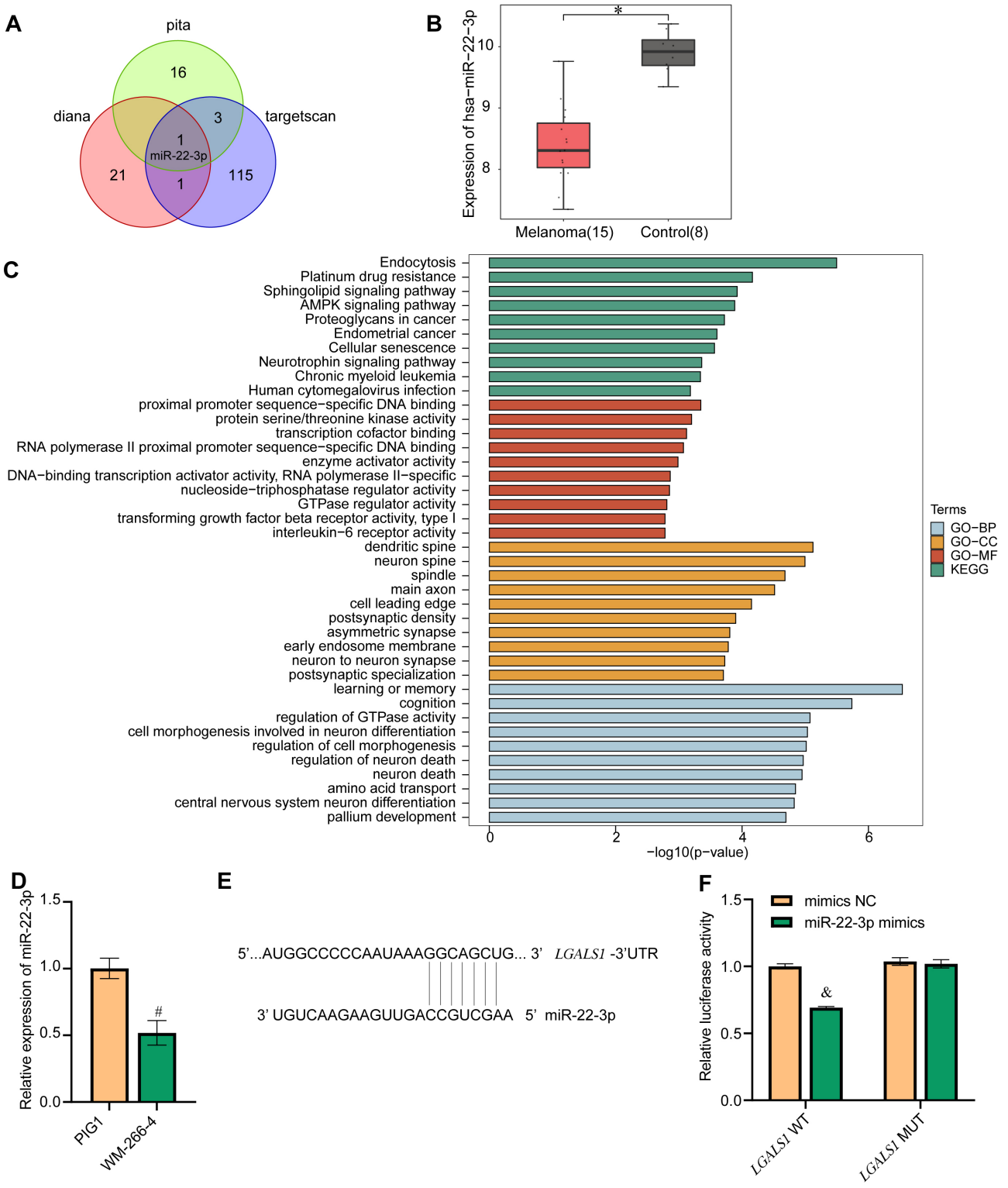

Fig. 4. Screening for LGALS1-interacting miRNAs. (A) Venn diagram of miRNAs identified to target LGALS1 in the pita, diana and targetscan databases. Only one DEM, miR-22-3p, was identified in all three databases. (B) Confirmation of miR-22-3p expression in the GEO database. (C) GO and KEGG functional enrichment analysis of miR-22-3p. Blue represents biological process (BP)-related functions in GO analysis. Yellow represents functions associated with cellular components (CC) in GO analysis. Red represents functions related to molecular function (MF) in GO analysis. Green represents KEGG functional analysis. (D) qRT-PCR showing miR-22-3p expression in cells. (E) Bioinformatics prediction of the *LGALS1* binding site for miR-22-3p. (F) Dual luciferase experiments were performed to verify the binding of *LGALS1* to miR-22-3p. $*p < 0.05$ vs. Control group, $^{\#}p < 0.05$ vs. PIG1 group, $^{\&}p < 0.05$ vs. mimics NC group.

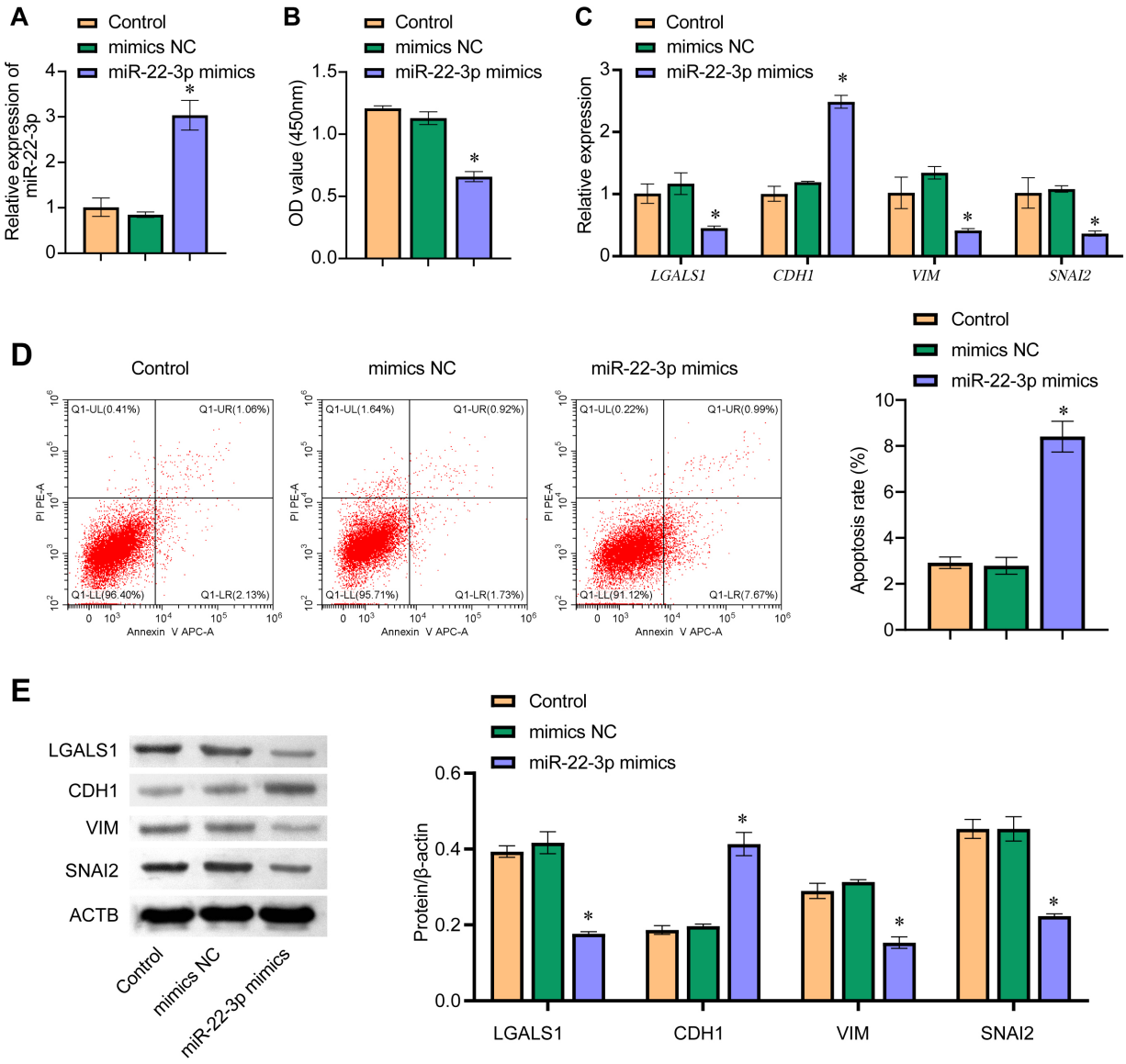

Fig. 5. miR-22-3p regulates EMT. (A) The expression level of miR-22-3p in WM-266-4 cells was evaluated by qRT-PCR. (B) CCK8 was used to determine WM-266-4 cell viability, with absorbance measured at 450 nm. (C) qRT-PCR was used to determine the cellular mRNA levels for *LGALS1*, *CDH1*, *VIM*, and *SNAI2*. (D) Detection of apoptosis by flow cytometry. (E) Cellular protein levels for LGALS1, CDH1, VIM, and SNAI2 were determined by western blot. *$p < 0.05$ vs. mimics NC group.

ings could provide a basis for the early prevention and treatment of subsequent melanoma. In the present study, we used bioinformatics analysis to identify multiple DEMs and DEGs in melanoma. The top 45 DEMs and top 90 DEGs were listed, and the expression levels of three genes (*LGALS1*, *CPXM1*, *APLNR*) and their association with patient survival were analyzed. The expression of these genes was confirmed to be higher in melanoma cells than in normal skin melanocytes. *LGALS1* was selected for additional follow-up studies.

It has been reported previously that *LGALS1* is associated with melanoma progression [21]. It is also known to induce EMT in ovarian, liver, and other cancer types [22–24]. However, a regulatory role for *LGALS1* on EMT in melanoma has not yet been reported. Our bioinformatics analyses predicted that *LGALS1* was a target for miR-22-3p binding. Dual luciferase experiments were performed to confirm this binding. We next analyzed the enrichment pathways of genes targeted by miR-22-3p. The BPs of these genes were concentrated in endocytosis and platinum resistance. Previous studies have also reported that miR-22-3p functions were enriched in endocytosis and platinum drug resistance [25,26]. For CC, genes targeted by miR-22-3p were enriched in proximal promoter sequence-specific DNA binding. Previous studies have shown that genes regulated by miR-22-3p are closely related to transcription fac-

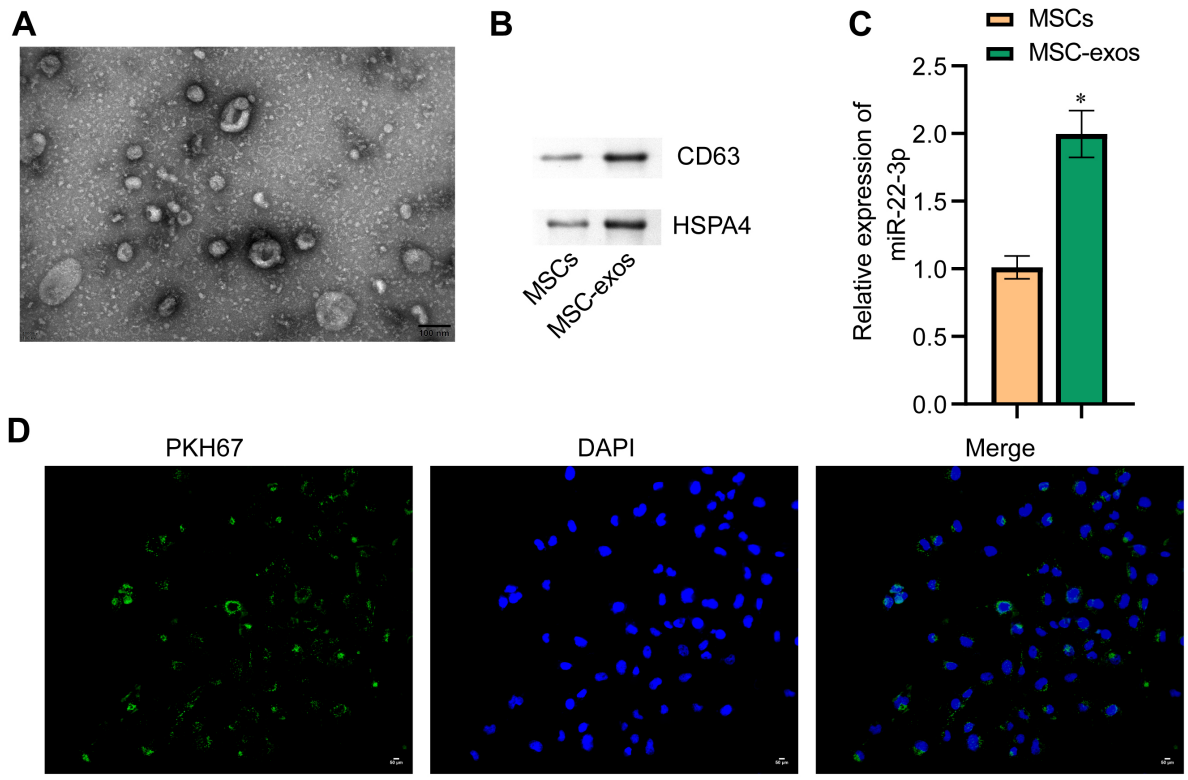

Fig. 6. Identification of MSC-EXOs and uptake of exosomes by melanoma cells. (A) Exosome morphology examined by TEM. The diameter of exosomes was about 50 nm (scale bar = 100 nm). (B) Western blot technique was used to determine protein levels for the exosome markers CD63 and HSPA4. (C) qRT-PCR was used to determine miR-22-3p levels in cells and exosomes. (D) PKH67 labeling was used to observe exosome uptake. Green represents exosomes, while blue represents cell nuclei. *$p < 0.05$ vs. MSCs.

tor activity RNA polymerase II core promoter proximal region sequence-specific binding [27]. For MF, miR-22-3p was associated with neuron spine, main axon, and cell leading edge. A prior study also showed that miR-22-3p could regulate the neuron spine [28]. For the KEGG pathway, miR-22-3p was involved in learning or memory, cognition. Another study reported a low level of miR-22-3p expression in the cerebrospinal fluid of exercisers [29]. After exercise, people fall into a state of fatigue, suggesting that miR-22-3p could regulate cognition by the brain. Various cancers including melanoma are regulated by EMT [30]. Wei *et al*. [8] showed that RNF128 affects the EMT process of melanoma by acting on the ubiquitination of CD44 and *CTTN* in melanoma cells through the Wnt/β-catenin signaling pathway. Wang *et al*. [31] showed that microRNA-214 downregulated *CADM1* in melanoma cells, thereby promoting EMT progression in melanoma. Together, these results suggest that the development of melanoma may be favored by the promotion of cellular EMT. By overexpressing miR-22-3p in WM-266-4 cells in the current study, we found that miR-22-3p could suppress EMT. Although the regulation of EMT by miR-22-3p has not previously been reported in melanoma, miR-22-3p is known to inhibit the progression of EMT in gastric cancer, colorectal cancer, lung adenocarcinoma, as well as other diseases [32–34].

After coating with miRNAs, exosomes are transported to cancer cells for action, thus effectively solving the difficult problem of target recognition [35]. Several studies have shown that miRNAs contained in exosomes secreted by MSCs can affect tumor cells [7]. Che *et al*. [36] showed that by encapsulating miR-143 within exosomes secreted by MSCs, *TFF3* could be regulated in prostate cancer cells, thereby inhibiting the migration and invasion of cancer cells. Naseri *et al*. [37] demonstrated that exosomes secreted by MSCs could also serve as delivery vehicles for small-molecule drugs such as anti-miR-142-3p. In the current study, exosomes secreted by MSCs were also used to study the delivery of miR-22-3p. By overexpressing miR-22-3p in MSCs, we found that exosomes could accurately and efficiently deliver miR-22-3p into WM-266-4 cells, thereby inhibiting the EMT of WM-266-4 cells. These results may provide a novel approach for the treatment of melanoma. However, future research will also need to investigate whether miR-22-3p and *LGALS1* can regulate the EMT of melanoma cells in animal studies and clinical trials, thereby inhibiting the progression of melanoma.

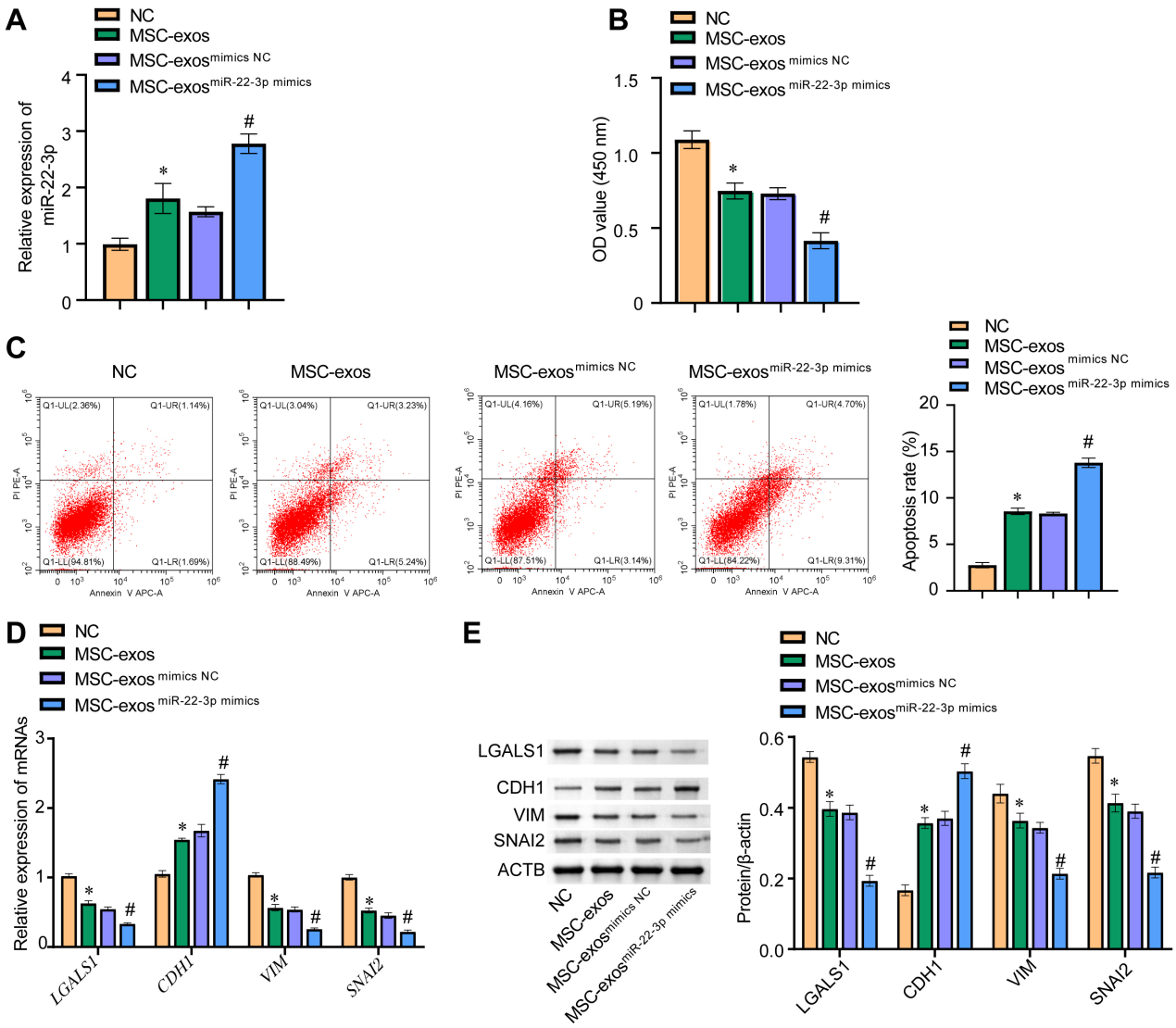

Fig. 7. miR-22-3p in MSC-exos inhibited EMT of melanoma cells by regulating LGALS1. (A) The expression level of miR-22-3p in WM-266-4 cells was evaluated by qRT-PCR. (B) The cck8 assay was used to evaluate the viability of WM-266-4 cells by measuring absorbance at 450 nM. (C) Cell apoptosis was detected by flow cytometry. (D) qRT-PCR was used to measure mRNA levels for *LGALS1*, *CDH1*, *VIM*, and *SNAI2* in WM-266-4 cells. (E) Western blot was used to determine the protein levels of LGALS1, CDH1, VIM, and SNAI2 in WM-266-4 cells. *$p < 0.05$ vs. NC. #$p < 0.05$ vs. MSC-exos $^{\text{mimics NC}}$ group.

5. Conclusions

Bioinformatics analysis was used to identify three genes (*LGALS1*, *CPXM1*, *APLNR*) that were differentially expressed in melanoma. miR-22-3p can target *LGALS1* and inhibit the EMT process in melanoma cells, thereby preventing the development of melanoma. Moreover, exosomes secreted by MSCs can be loaded with miR-22-3p, thus regulating the EMT process in melanoma cells.

Data Availability Statement

All data included in this study are available upon request by contact with the corresponding author.

Author Contributions

HL, TC, BT—Conceptualization, Methodology, Software, Supervision; YC, YF—Data curation, Validation, Writing- Original draft preparation, Writing- Reviewing and Editing; LL—Visualization, Investigation. All the authors above approved the version of the manuscript to be published.

Ethics Approval and Consent to Participate

Not applicable.

Acknowledgment

Not applicable.

Funding

This research received a funding from Natural Science Foundation of Hunan Province of China (Grant/Award Number: 2020JJ4533).

Conflict of Interest

The authors declare no conflict of interest.

Supplementary Material

Supplementary material associated with this article can be found, in the online version, at https://doi.org/10.31083/j.fbl2709275.

References

[1] Davis LE, Shalin SC, Tackett AJ. Current state of melanoma diagnosis and treatment. Cancer Biology and Therapy. 2019; 20: 1366–1379.

[2] Jenkins RW, Fisher DE. Treatment of Advanced Melanoma in 2020 and beyond. Journal of Investigative Dermatology. 2021; 141: 23–31.

[3] Lee KA, Nathan P. Cutaneous Melanoma - A Review of Systemic Therapies. Acta Dermato-Venereologica. 2020; 100: adv00141.

[4] Kabekkodu SP, Shukla V, Varghese VK, D' Souza J, Chakrabarty S, Satyamoorthy K. Clustered miRNAs and their role in biological functions and diseases. Biological Reviews of the Cambridge Philosophical Society. 2018; 93: 1955–1986.

[5] Yang F, Ning Z, Ma L, Liu W, Shao C, Shu Y, *et al*. Exosomal miRNAs and miRNA dysregulation in cancer-associated fibroblasts. Molecular Cancer. 2017; 16: 148.

[6] Sun Z, Shi K, Yang S, Liu J, Zhou Q, Wang G, *et al*. Effect of exosomal miRNA on cancer biology and clinical applications. Molecular Cancer, 2018; 17: 147.

[7] Weng Z, Zhang B, Wu C, Yu F, Han B, Li B, *et al*. Therapeutic roles of mesenchymal stem cell-derived extracellular vesicles in cancer. Journal of Hematology and Oncology. 2021; 14: 136.

[8] Wei C, Zhu M, Yang Y, Zhang P, Yang X, Peng R, *et al*. Downregulation of RNF128 activates Wnt/β-catenin signaling to induce cellular EMT and stemness via CD44 and CTTN ubiquitination in melanoma. Journal of Hematology and Oncology. 2019; 12: 21.

[9] Romano G, Kwong LN. Kwong, miRNAs, Melanoma and Microenvironment: An Intricate Network. International Journal of Molecular Sciences. 2017; 18: 2354.

[10] Pedri D, Karras P, Landeloos E, Marine J, Rambow F. Epithelial-to-mesenchymal-like transition events in melanoma. the FEBS Journal. 2022; 289: 1352–1368.

[11] Tang Y, Durand S, Dalle S, Caramel J. EMT-Inducing Transcription Factors, Drivers of Melanoma Phenotype Switching, and Resistance to Treatment. Cancers. 2020; 12: 2154.

[12] Hoek KS, Eichhoff OM, Schlegel NC, Döbbeling U, Kobert N, Schaerer L, *et al*. In vivo switching of human melanoma cells between proliferative and invasive states. Cancer Research. 2008; 68: 650–656.

[13] Rambow F, Rogiers A, Marin-Bejar O, Aibar S, Femel J, Dewaele M, *et al*. Toward Minimal Residual Disease-Directed Therapy in Melanoma. Cell. 2018; 174: 843–855.e19.

[14] Verfaillie A, Imrichova H, Atak ZK, Dewaele M, Rambow F, Hulselmans G, *et al*. Decoding the regulatory landscape of melanoma reveals TEADS as regulators of the invasive cell state. Nature Communications. 2015; 6: 6683.

[15] Chen L, Heikkinen L, Wang C, Yang Y, Sun H, Wong G. Trends in the development of miRNA bioinformatics tools. Briefings in Bioinformatics. 2019; 20: 1836–1852.

[16] Pearlman RL, Montes de Oca MK, Pal HC, Afaq F. Potential therapeutic targets of epithelial–mesenchymal transition in melanoma. Cancer Letters. 2017; 391: 125–140.

[17] Liu S, Xie X, Lei H, Zou B, Xie L. Identification of Key circRNAs/lncRNAs/miRNAs/mRNAs and Pathways in Preeclampsia Using Bioinformatics Analysis. Medical Science Monitor. 2019; 25: 1679–1693.

[18] Yang G, Zhang Y, Yang J. Identification of Potentially Functional CircRNA-miRNA-mRNA Regulatory Network in Gastric Carcinoma using Bioinformatics Analysis. Medical Science Monitor. 2019; 25: 8777–8796.

[19] Yang D, He Y, Wu B, Deng Y, Wang N, Li M, *et al*. Integrated bioinformatics analysis for the screening of hub genes and therapeutic drugs in ovarian cancer. Journal of Ovarian Research. 2020; 13: 10.

[20] Wang LX, Wan C, Dong ZB, Wang BH, Liu HY, Li Y. Integrative Analysis of Long Noncoding RNA (lncRNA), microRNA (miRNA) and mRNA Expression and Construction of a Competing Endogenous RNA (ceRNA) Network in Metastatic Melanoma. Medical Science Monitor. 2019; 25: 2896–2907.

[21] Rizzolio S, Corso S, Giordano S, Tamagnone L. Autocrine Signaling of NRP1 Ligand Galectin-1 Elicits Resistance to BRAF-Targeted Therapy in Melanoma Cells. Cancers. 2020; 12: 2218.

[22] Liu Y, Wu L, Ao H, Zhao M, Leng X, Liu M, *et al*. Prognostic implications of autophagy-associated gene signatures in non-small cell lung cancer. Aging. 2019; 11: 11440–11462.

[23] Zhang PF, Li KS, Shen YH, Gao PT, Dong ZR, Cai JB, *et al*. Galectin-1 induces hepatocellular carcinoma EMT and sorafenib resistance by activating FAK/PI3K/AKT signaling. Cell Death & Disease. 2016; 7: e2201.

[24] Zhu J, Zheng Y, Zhang H, Liu Y, Sun H, Zhang P. Galectin-1 induces metastasis and epithelial-mesenchymal transition (EMT) in human ovarian cancer cells via activation of the MAPK JNK/p38 signalling pathway. American Journal of Translational Research. 2019; 11: 3862–3878.

[25] Dang Y, Zhao S, Qin Y, Han T, Li W, Chen Z. MicroRNA-22-3p is down-regulated in the plasma of Han Chinese patients with premature ovarian failure. Fertility and Sterility. 2015; 103: 802–807.e1.

[26] Qi X, Yu C, Wang Y, Lin Y, Shen B. Network vulnerability-based and knowledge-guided identification of microRNA biomarkers indicating platinum resistance in high-grade serous ovarian cancer. Clinical and Translational Medicine. 2019; 8: 28.

[27] Vastrad B, Vastrad C, Godavarthi A, Chandrashekar R. Molecular mechanisms underlying gliomas and glioblastoma pathogenesis revealed by bioinformatics analysis of microarray data. Medical Oncology. 2017; 34: 182.

[28] Li B, Wang Z, Yu M, Wang X, Wang X, Chen C, *et al*. MiR-22-3p enhances the intrinsic regenerative abilities of primary sensory neurons via the CBL/p-EGFR/p-STAT3/GAP43/p-GAP43 axis. Journal of Cellular Physiology. 2020; 235: 4605–4617.

[29] Baraniuk JN, Shivapurkar N. Exercise – induced changes in cerebrospinal fluid miRNAs in Gulf War Illness, Chronic Fatigue Syndrome and sedentary control subjects. Scientific Reports. 2017; 7: 15338.

[30] Sarkar D, Leung EY, Baguley BC, Finlay GJ, Askarian-Amiri ME. Epigenetic regulation in human melanoma: past and future. Epigenetics. 2015; 10: 103–121.

[31] Wang SJ, Li WW, Wen CJ, Diao YL, Zhao TL. MicroRNA-214 promotes the EMT process in melanoma by downregulating CADM1 expression. Molecular Medicine Reports. 2020; 22: 3795–3803.

[32] Zhang W, Zhan F, Li D, Wang T, Huang H. RGMB-as1/miR-22-

3p/NFIB axis contributes to the progression of gastric cancer. Neoplasma. 2020; 67: 484–491.
[33] Hu X, Xing W, Zhao R, Tan Y, Wu X, Ao L, *et al*. HDAC2 inhibits EMT-mediated cancer metastasis by downregulating the long noncoding RNA H19 in colorectal cancer. Journal of Experimental and Clinical Cancer Research. 2020; 39: 270.
[34] Zhou J, Zhang S, Chen Z, He Z, Xu Y, Li Z. CircRNA-ENO1 promoted glycolysis and tumor progression in lung adenocarcinoma through upregulating its host gene ENO1. Cell Death and Disease. 2019; 10: 885.
[35] Duan H, Liu Y, Gao Z, Huang W. Recent advances in drug delivery systems for targeting cancer stem cells. Acta Pharmaceutica Sinica B. 2021; 11: 55–70.
[36] Che Y, Shi X, Shi Y, Jiang X, Ai Q, Shi Y, *et al*. Exosomes Derived from miR-143-Overexpressing MSCs Inhibit Cell Migration and Invasion in Human Prostate Cancer by Downregulating TFF3. Molecular Therapy - Nucleic Acids. 2019; 18: 232–244.
[37] Naseri Z, Oskuee RK, Jaafari MR, Forouzandeh Moghadam M. Exosome-mediated delivery of functionally active miRNA-142-3p inhibitor reduces tumorigenicity of breast cancer in vitro and in vivo. International Journal of Nanomedicine. 2018; 13: 7727–7747.